Acknowledgments

We gratefully acknowledge Sacha Parneix and Ewald Lutum (Alstom Power Technology, Baden, Switzerland) for providing the heat transfer equations for computing the mass flow and the thermal boundary conditions. We also thank Nikolaus Hansen (Technical University of Berlin) for many useful discussions about the covariance matrix adaption–evolution strategy.

References

[1]Schwefel, H.-P., *Evolution and Optimum Seeking*, Wiley, New York, 1995, pp. 105–164.

[2]Hansen, N., and Ostermeier, A., "Convergence Properties of Evolution Strategies with the Derandomized Covariance Matrix Adaptation: The $(\mu/\mu_I, \lambda)$-CMA-ES," *Proceedings of the 5th European Congress on Intelligent Techniques and Soft Computing (EUFIT'97)*, Verlag Mainz, Aachen, Germany, 1997, pp. 650–654.

[3]McGreehan, W. F., and Schotsch, M. J., "Flow Characteristics of Long Orifices with Rotation and Corner Radiusing," American Society of Mechanical Engineers, ASME Paper 87-GT-162, June 1987.

[4]Goldstein, R. J., "Film Cooling," *Advances in Heat Transfer*, Vol. 7, 1971, pp. 321–379.

[5]Seller, J. P., "Gaseous Film Cooling with Multiple Ejection Stations," *AIAA Journal*, Vol. 1, No. 9, 1963, pp. 2154–2156.

[6]STAR-CD User Manual, Computational Dynamics, Ltd., London, Dec. 1997.

A. Chattopadhyay
Associate Editor

Role of Tip and Edge Geometry on Vortex Asymmetry

T. T. Lim,* K. B. Lua,† and S. C. Luo*
National University of Singapore, Singapore 119260, Republic of Singapore

Introduction

In the late 1960s, Bird[1] investigated the flow over a delta wing at high incidence and noted the asymmetric lifting of the apex or tip vortices from the wing. However, a similar and more recent investigation by Stahl et al.[2] found the corresponding vortices to be symmetrical instead. Stahl et al.[2] and Ericsson[3] attributed the conflicting results to the different tip conditions of the two delta wings. They pointed out that the delta wing of Stahl et al.[2] had a triangular tip with sharp edges, whereas the one used by Bird[1] had a conical tip, which presumably was subjected to the same source of vortex asymmetry as an ogive–cylinder or a cone. The preceding explanation implies that the nose geometry plays a crucial role in determining the orientation of the tip vortices. To determine whether this is also true for other slender plates, we perform a series of flow visualization studies on an ogive-shaped plate at a high angle of attack. As the name implies, the plate has the same profile as the center plane of an ogive–cylinder in much the same way that a delta wing has the same profile as the center plane of an axisymmetric cone. This particular geometry is chosen for study because, apart from addressing the issue of vortex asymmetry, it enables comparison with previous experimental studies of the ogive–cylinder.[4,5]

Experimental Apparatus and Procedures

The experiments were performed in the National University of Singapore's 0.4×0.4 m test section water channel using a dye visualization technique. A total of four ogive-shaped plates were fabricated, with different tip and edge conditions. All of the plates are 24 mm (D) wide and 3 mm thick and have the same tip finess ratio, that is, $3.5D$, as the ogive–cylinder used in our earlier study (Fig. 1a). In the first plate or model, the edges were chamfered at 45 deg and extended all of the way to the apex of the model. For ease of reference, it is referred to as sharp tip and sharp edges (STSE) (Fig. 1b). This model has the same tip and edge conditions as the delta wing used by Stahl et al.[2] In the second model, the edges were also chamfered, but the apex has an axisymmetric ogive tip of length 5.27 mm (or $0.22D$) (Fig. 1c). This model is referred to as ogive tip and sharp edges (OTSE). The third model has the same ogive tip as the OTSE model, but the edges are rounded with a radius of 1.5 mm (half of the model thickness) (Fig. 1d). This model is referred to as ogive tip and round edges (OTRE) and is the counterpart of the delta wing of Bird.[1] The last model has the same apex geometry as STSE and the round edges of OTRE. Accordingly, it is referred to as sharp tip and round edges (STRE) (Fig. 1e). These four models provide all of the possible combinations of sharp and rounded edge and tip geometries.

In the actual experiment, the base of each ogive-shaped plate was supported by a mechanism above the water surface, and the plate pitched downward and pierced through the free surface. This arrangement allowed the tip of the plate to be farthest away from the free surface, hence ensuring that free surface effects, if any, were kept to a minimum. Before each run, a height gauge was used to align painstakingly the model with the centerline of the test section and ensure that the yaw and roll angles were zero with respect to the freestream. This laborious process was deemed necessary because the accuracy of the results depended critically on the accuracy of the model alignment. To visualize the flow, dye was released slowly and with minimum disturbance to the flow from the two dye ports located at 20 mm from the apex and slightly on the leeward side of the model. In all cases, the groove that carries the stainless tubing for the dye injection was filled with epoxy resin and carefully shaped to match the profile of the body. For the purpose of distinguishing the two tip vortices, red dye was released from the port side of the model, and blue dye was released from the mirror image port on the starboard side. The operating Reynolds number based on the width of the plate was approximately 3.2×10^3.

The flow patterns were captured from the bottom and side of the test section using two charge-coupled device (CCD) video cameras and a Nikon F3 single-lens-reflex still camera equipped with a Nikkor 50-mm lens. To avoid the effect of parallax, extreme care was taken when aligning the camera with respect to the model. To conform with the common practice of flow direction from left to right, the side views of the captured images have been rotated by 180 deg, as shown in Figs. 2 and 3.

Results and Discussion

In Fig. 2, the side and the plan views of the tip vortices for the four ogive-shaped plates tested are displayed. Although the plates were tested for a range of moderately high angles of attack α from 40 to 60 deg, only the results for $\alpha = 40$ deg are presented because the salient flow features for the other angles are essentially the same.

Figure 2a shows the results for the STSE plate at $\alpha = 40$ deg. It is obvious from the dye patterns that the tip vortices were symmetrical up to the locations of the apparent vortex breakdown. The existence of the vortex breakdown is supported by the video images, which clearly show a region of recirculating flow immediately after the dye core has undergone sudden enlargement. It is not clear what caused the vortices to breakdown at the different positions, but a similar phenomenon has often been observed on the tip vortices from delta wings at high angles of attack.[2]

In Fig. 2b, the results for OTSE model are displayed. Here, it can be seen that the vortices remained symmetrical up to the vortex breakdown positions despite the model having an axisymmetric tip. This flow behavior is contrary to the speculation by Stahl et al.[2] and Ericcson,[3] which suggested that the vortices should be asymmetric if the tip is rounded. That the vortices were not asymmetric indicated that the axisymmetric tip may not be solely responsible for the vortex asymmetry. The sharp edges may have played an equally influential

Received 27 August 1999; revision received 31 August 2000; accepted for publication 13 September 2000.

*Associate Professor, Department of Mechanical and Production Engineering, 10 Kent Ridge Crescent.

†Research Engineer, Department of Mechanical and Production Engineering, 10 Kent Ridge Crescent.

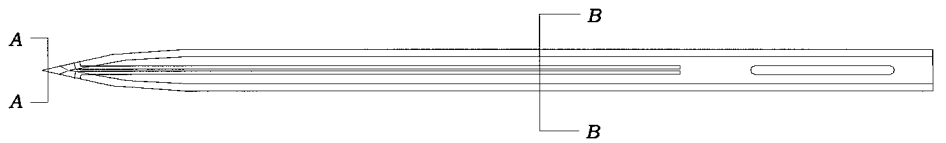

a) Schematic drawings of ogive-shaped plate

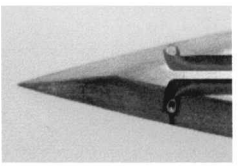

Picture of the nose

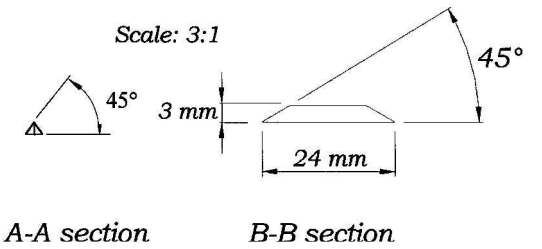

b) STSE

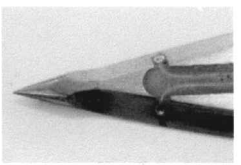

Picture of the nose

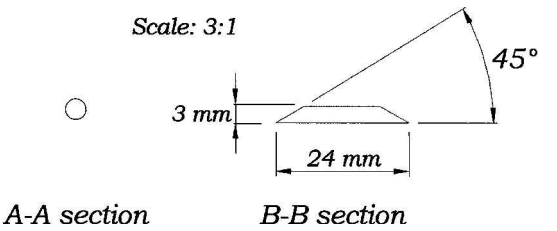

c) OTSE

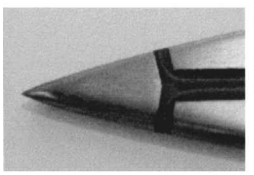

Picture of the nose

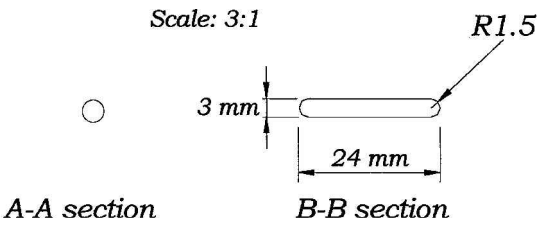

d) OTRE

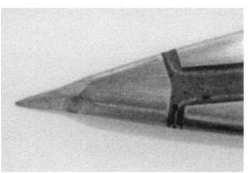

Picture of the nose

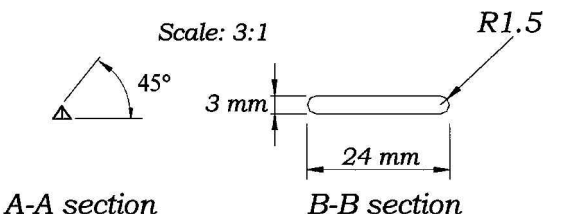

e) STRE

Fig. 1 Ogive-shaped plates.

role by restricting the movement of the flow separation position, thus inhibiting the vortices from becoming asymmetric.

When the sharp edges of OTSE model in Fig. 2b was replaced by the round edges, that is, the OTRE model, the vortices switched from the symmetrical to the asymmetrical state as is clearly depicted in Fig. 2c. Note that the small extent of the vortex asymmetry observed here is consistent with the experimental results of Stahl[6] and the computational work of Fiddes and Williams,[7] which show that the extent of vortex asymmetry decreases as the model becomes flatter. Because this model is the counterpart of the delta wing used by Bird,[1] it is not surprising that the present finding is consistent with those results.

When the ogive tip in Fig. 2c was replaced by a sharp triangular tip as shown in the STRE model, the extent of the vortex asymmetry increased considerably, with the starboard vortex yawing away from the body much earlier than the port side vortex [Figs. 2d (i) and 2d (ii))]. This occurred despite the model having a triangular tip, which, according to the conjecture by Stahl et al.[2] and Ericcson,[3] should produce symmetrical vortices. Note that the background of the pictures in Figs. 2d (ii) and 4b (ii) has been enhanced to give a better contrast of the dye pattern.

An inevitable question arises as to whether plate misalignment may have caused the vortices in Figs. 2c and 2d to become asymmetric. To ensure that this is not the case, the plates were also tested at a low angle of attack of 30 deg, and in all cases the vortices were found to be symmetrical. This finding is consistent with the previous published results on an ogive–cylinder and conical body showing symmetrical tip vortices when α is smaller than the onset angle of vortex asymmetry. If the plates had been misaligned, one would have expected to see some degree of vortex asymmetry as in Figs. 2c and 2d at a low angle of attack.

From the preceding findings, it is clear that axisymmetric ogive tip is not solely responsible for the vortex asymmetry, at least for the ogive-shaped plates. The flow separation positions also depend critically on edge geometry. If the separation positions are fixed by the sharp edges as in the models STSE and OTSE, then vortex asymmetry will not occur, irrespective of the tip condition. Likewise, having a triangular tip alone is no guarantee that the vortices will become symmetrical as the STRE model has shown; the plate must also have sharp edges.

To determine whether vortex asymmetry on the ogive-shaped plates was also caused by vortex crowding as in the case of the

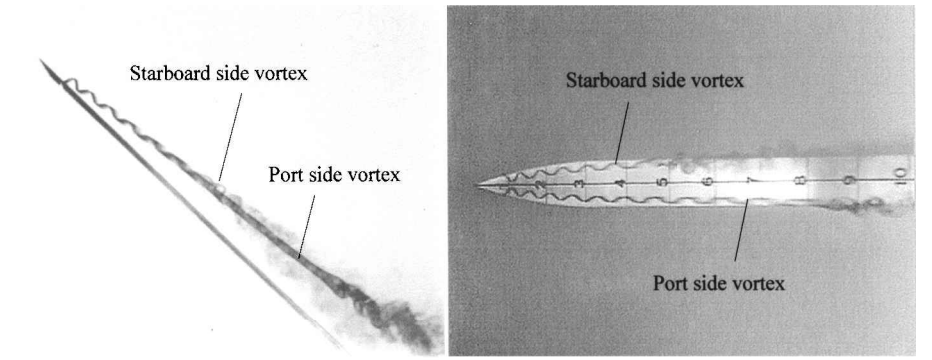

(i) side view (ii) plan view

a) STSE

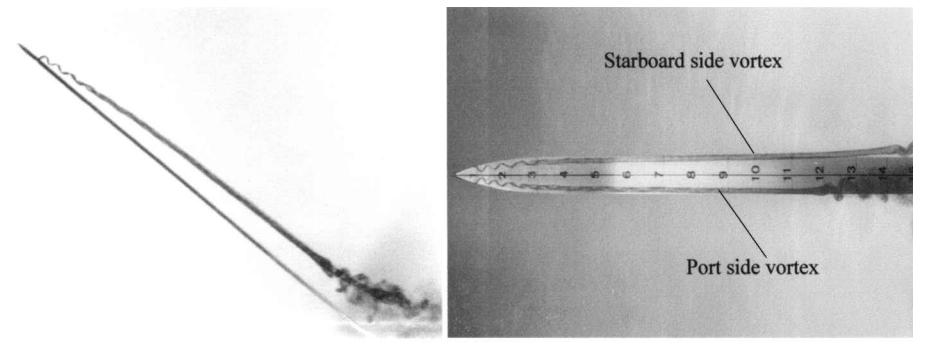

(i) side view (ii) plan view

b) OTSE

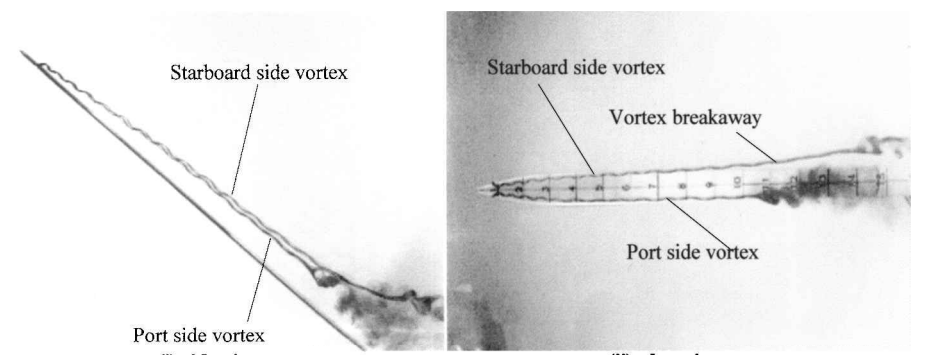

(i) side view (ii) plan view

c) OTRE

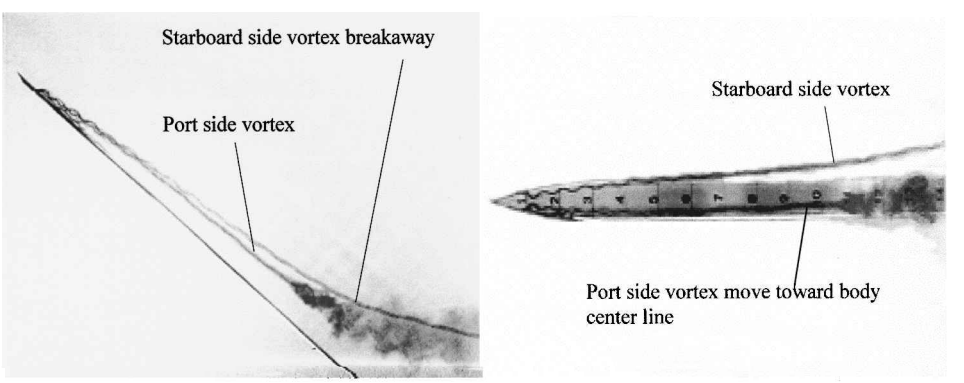

(i) side view (ii) plan view

d) STRE

Fig. 2 Dye pattern of flow past ogive-shaped plates at $\alpha = 40$ deg to the oncoming flow from left to right. Note the presence of symmetrical vortices in parts a and b and asymmetrical vortices in parts c and d.

ogive–cylinder, a fin or strake similar to that used by Ng[8] was incorporated on the OTRE and STRE models because they were the only ones that produced asymmetric vortices. The dimensions of the fin are indicated in Fig. 3, with the fin installed such that its tip coincides with the tip of the plate. It is clear from the results in Fig. 4 that the fin had indeed caused the vortices to switch from an asymmetric to a symmetric state as Ng has previously found (see also Refs. 9 and 10). Except for the presence of fine-scale structures on the vortices, there was no noticeable vortex breakaway from the body [compare Figs. 4a (i) and 4a (ii) with Figs. 2c (i) and 2c (ii), and Figs. 4b (i) and 4b (ii) with Figs. 2d (i) and 2d (ii)]. This study clearly shows that the phenomenon of vortex crowding is not restricted to an axisymmetric or conical tip, but can also occur for a triangular tip. Moreover, that the fin suppressed the vortex asymmetry on the STRE and OTRE models implies that in the absence of the vortex crowding, the influence of a micro surface imperfection on the round edges of the models is probably not very significant. This finding is in line with the suggestion by Ng[8] that vortex crowding has an amplifying effect on the perturbation imposed by the micro surface imperfection on the body.

Based on the present findings, it is reasonable to suggest that the symmetric vortices observed by Stah et al.[2] could have been controlled by the sharp edges, which restricted the movement of the separation positions. Similarly, the asymmetric lifting of the vortices seen by Bird[1] could have been enhanced by the round edges (in combination with the possible effect of the micro surface imperfection), which allowed the movement of the flow separation positions.

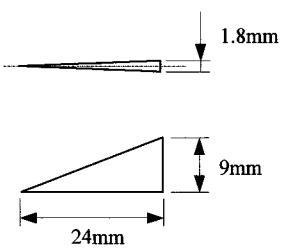

Fig. 3 Dimensions of the vortex separating fin or strake.

Conclusions

Experimental investigations on four ogive-shaped plates have been carried out. The results strongly suggest that an axisymmetric ogive tip is not solely responsible for the phenomenon of vortex asymmetry. The edge geometry also plays a crucial role.

The fin or strake investigation on the OTRE and STRE models shows that the phenomenon of vortex crowding is not limited to the ogive tip and can also occur on a triangular tip.

As a final remark, we would like to stress that although the tip geometry may not be wholly responsible for the vortex asymmetry (at least for the ogive-shaped plate), it does not mean that it has no effect on the force distribution. Previous investigations on a slender body of revolution showed that the tip condition plays a significant role in the overall force distribution of the body.

References

[1]Bird, J. D., "Tuft-Grid Surveys at Low Speed for Delta Wings," NASA TN D-5045, Feb. 1969.

[2]Stahl, W. H., Mohmood, M., and Asghar, A., "Experimental Investigations of the Vortex Flow on Delta Wings at High Incidence," *AIAA Journal*, Vol. 30, No. 4, 1992, pp. 1027–1032.

[3]Ericsson, L. E., "Sources of High Alpha Vortex Asymmetry at Zero Sideslip," *Journal of Aircraft*, Vol. 29, No. 6, 1992, pp. 1086–1090.

[4]Luo, S. C., Lim, T. T., Lua, K. B., Chia, H. T., Goh, E. K. R., and Ho, Q. W., "Flowfield Around Ogive/Elliptic-Tip Cylinder at High Angle of Attack," *AIAA Journal*, Vol. 36, No. 10, 1998, pp. 1778–1787.

[5]Lee, A. S., Luo, S. C., Lim, T. T., Lua, K. B., and Goh, E. K. R., "Side Force on an Ogive Cylinder: Effect of Control Devices," *AIAA Journal*, Vol. 38, No. 3, 2000, pp. 385–388.

[6]Stahl, W. H., "Experimental Investigations of Asymmetric Vortex Flows Behind Elliptic Cones at Incidence," *AIAA Journal*, Vol. 31, No. 5, 1993, pp. 966–968.

[7]Fiddes, S. P., and Williams, A. L., "Recent Developments in the Study of Separated Flows Past Slender Bodies at Incidence," *Proceedings of Symposium on the Prediction and Exploitation of Separated Flow*, Royal Aeronautical Society, London, 1989, pp. 31.1–31.7.

[8]Ng, T. T., "Effect of a Single Strake on the Forebody Vortex Asymmetry," *Journal of Aircraft*, Vol. 27, No. 9, 1990, pp. 844–846.

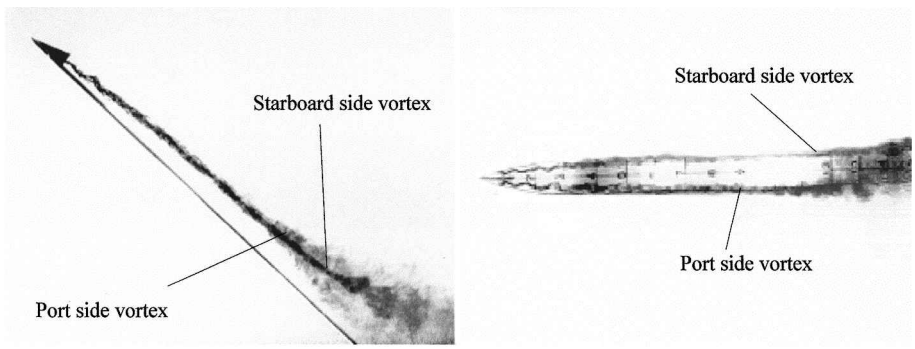

(i) side view **(ii) plan view**

a) OTRE

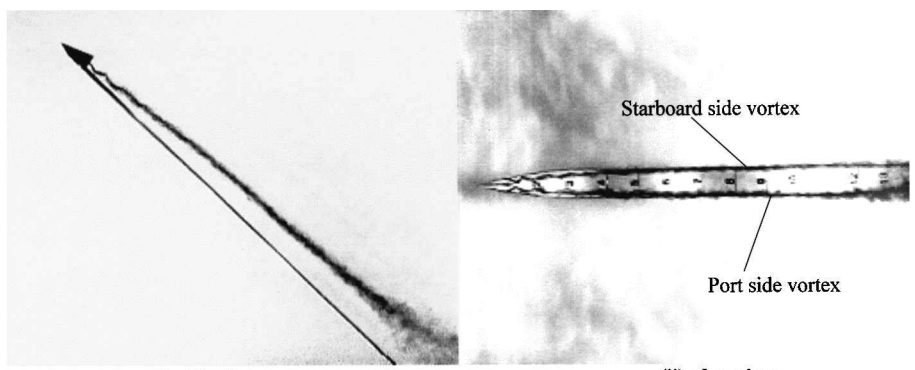

(i) side view **(ii) plan view**

b) STRE

Fig. 4 Dye pattern of flow past selected ogive-shaped plates with fin at $\alpha = 40$ deg to the oncoming flow from left to right. Note that the incorporation of the fin has transformed the asymmetric vortices in Figs. 2c and 2d to the symmetrical configuration shown here.

[9]Degani, D., "Numerical Study of the Effect of Geometrical Disturbances on Vortex Asymmetry," *AIAA Journal*, Vol. 29, No. 4, 1991, pp. 560–566.

[10]Degani, D., "Instability of Flows over Bodies at Large Incidence," *AIAA Journal*, Vol. 30, No. 1, 1992, pp. 94–100.

J. C. Hermanson
Associate Editor

In-Plane Vibrations of Nonuniform Circular Beams

Sen Yung Lee* and Jeng Chung Chao†
National Cheng-Kung University, Tainan 701, Taiwan, Republic of China

Nomenclature

$A(s)$	=	cross-sectional area of the beam
$E(s)$	=	Young's modulus of the material
F_{rv}	=	force per unit arc length in the r direction caused by the flexural deflection parameter V
$F_{\theta v}$	=	force per unit arc length in the θ direction caused by the flexural deflection parameter V
$I_z(s)$	=	area moment of inertia of the beam section about the z axis
L	=	total length of the neutral axis of the beam
R	=	radius of the curved beam
s	=	arc length variable, $s = R\theta$
$U(s)$	=	longitudinal displacement parameter
u	=	neutral axis displacement of the beam in the θ direction
$V(s)$	=	flexural displacement parameter
v	=	neutral axis displacement of the beam in the r direction
β	=	angular frequency of the in-plane vibration
$\rho(s)$	=	mass per unit volume of the beam

Introduction

CURVED-BEAM structures have been used in many aerospace, mechanical, and civil engineering applications such as curved wires in missile-guidance floated gyroscopes, stiffeners in aircraft structures, turbomachinery blades, curved girder bridges, brake shoes within drum brakes, spring design, and tire dynamics. It can also be used as a simplified model of a shell structure. Research in this area can be traced back to the 19th century.[1,2] An interesting review can be found in the review papers by Markus and Nanasi,[3] Laura and Maurizi,[4] Childamparam and Leissa,[5] and Auciello and De Rosa.[6]

In general, the out-of-plane and the in-plane vibrations of a general plane curved beam are coupled. However, if the cross section of the curved beam is doubly symmetric and the thickness of the beam is small in comparison with the radius of the beam, then the out-of-plane and the in-plane vibrations are independent.[2,7]

Many investigators have studied the in-plane vibrations of curved beams. The associated governing differential equations are two coupled differential equations in the flexural and the longitudinal displacements. If the beam is uniform, then the coefficients of the differential equations are constants. After some simple arithmetic operations the two coupled differential equations can be reduced into a sixth-order ordinary differential equation with constant coefficients in the flexural displacement.[2] Hence the problem can be solved by different analytical methods, and the exact solutions can be obtained.[2,8–10] However, it is not the case for the nonuniform beams.

Received 25 January 2000; revision received 24 July 2000; accepted for publication 27 July 2000.

*Professor, Mechanical Engineering Department; sylee@mail.ncku.edu.tw.

†Graduate Student, Mechanical Engineering Department.

Because of the complexity in the coefficients of the governing differential equations, the two-coupled differential equations have never been uncoupled and reduced into sixth-order ordinary differential equations. Exact solutions for the curved nonuniform beam problem are only found in the work done by Suzuki and Takahashi,[11] who gave an exact series solution to the beams with the same boundary conditions at both ends. Nevertheless, their method has difficulty in handing the problems with other kind of boundary conditions. Hence, the problems were studied mainly by approximated methods such as the Rayleigh–Ritz method,[12] the Galerkin method,[13] the transfer matrix method,[14] the discrete Green function method,[15] and the asymptotic analysis of the equations of free vibrations.[16]

In this Note, by introducing two physical parameters, the analysis is simplified, and the explicit relations between the flexural displacement and the longitudinal displacement of the system are derived. With these explicit relations the coupled governing characteristic differential equations can be uncoupled and reduced to sixth-order ordinary differential equations with variable coefficients in the flexural displacement. In addition, by employing the explicit relations, one only has to measure one variable instead of two simultaneously while performing experimental studies of curved beams. Hence, it greatly reduces the difficulty in experimental measurements.

When the radius of a curved beam becomes infinite, the curved beams reduces to a straight beam. Consequently, the sixth-order ordinary differential equation in the flexural displacement should reduce to a fourth-order ordinary differential equation. However, it is not possible to perform this limiting process from the reduced sixth-order ordinary differential equation for the beam,[2] and the limiting study had never been successfully explored before. In this Note, by employing the explicit relations, a successful limiting study is revealed.

Coupled Governing Differential Equations

Consider the in-plane vibrations of nonuniform curved beams of constant radius R and doubly symmetric cross section, as shown in Fig. 1. If the thickness of the beam is small in comparison with the radius of the beam, without considering the shear deformation, the rotary inertia, and the warping effects the governing differential equations for the in-plane vibrations are two coupled differential equations in terms of the flexural and the longitudinal displacements.[7]

For time-harmonic in-plane vibrations of curved beams with angular frequency β, one assumes

$$u(s, t) = U(s)e^{i\beta t} \tag{1}$$

$$v(s, t) = V(s)e^{i\beta t} \tag{2}$$

The two coupled governing characteristic differential equations of the system are

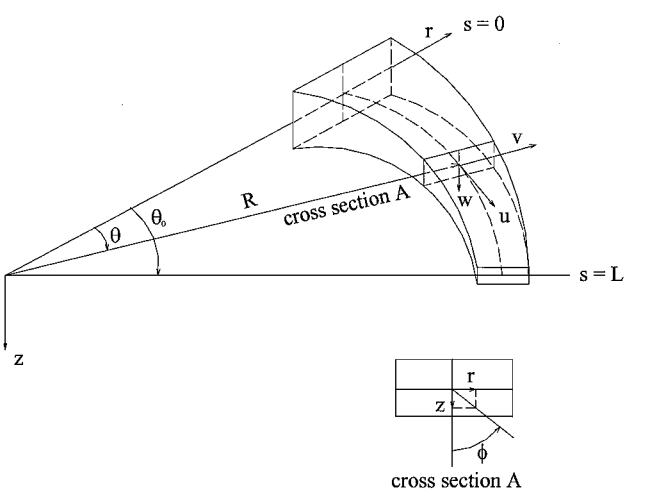

Fig. 1 Geometry and coordinate system of a curved nonuniform beam of constant radius.